CANCER

Xenogenization of tumor cells by fusogenic exosomes in tumor microenvironment ignites and propagates antitumor immunity

Gi Beom Kim[1,2]*, Gi-Hoon Nam[1,2]*, Yeonsun Hong[1,2], Jiwan Woo[3], Yakdol Cho[3], Ick Chan Kwon[1,2], Yoosoo Yang[2,4]†, In-San Kim[1,2]†

Many cancer patients not responding to current immunotherapies fail to produce tumor-specific T cells for various reasons, such as a lack of recognition of cancer cells as foreign. Here, we suggest a previously unidentified method for xenogenizing (turning self to non-self) tumors by using fusogenic exosomes to introduce fusogenic viral antigens (VSV-G) onto the tumor cell surface. We found that xenogenized tumor cells were readily recognized and engulfed by dendritic cells; thereby, tumor antigens were efficiently presented to T lymphocytes. Moreover, exosome–VSV-G itself acts as a TLR4 agonist and stimulates the maturation of dendritic cells, leading to $CD8^+$ T cell cross-priming. The administration of these exosomes in multiple tumor mouse models xenogenized tumor cells, resulting in tumor growth inhibition. The combinatorial treatment with anti–PD-L1 exhibited complete tumor regression (30%) and better long-term overall survival. These results suggest that tumor xenogenization by fusogenic exosomes provides a previously unidentified a novel strategy for cancer immunotherapy.

INTRODUCTION

Immune checkpoint blockades have revolutionized the treatment of patients with several types of malignancies, but only a subset of patients responds to these therapies (*1*). To increase the response rates to current immunotherapies, researchers have sought to modify tumor cells to render them more immunogenic. In particular, because many tumors with high mutational burdens are predicted to improve clinical benefit to immune checkpoint blockades (*2*), altering the tumor cell phenotypes may be a useful means to elevate tumor immunogenicity.

The term "xenogenization" refers to the use of pathogenic antigen, increasing the likelihood that a cancer cell will be recognized as non-self or foreign by the host immune system. The introduction of pathogen-associated molecular patterns (PAMPs) onto cancer cells through viral infection has been called "artificial" xenogenization (*3*). Specifically, infection of tumor cells with a nonlytic budding virus causes an acquisition of new foreign virus-specific proteins in the host and induces an immunological regression of tumors (*4*). In addition, xenogenization can also be induced indirectly by chemicals, triazene compounds, which have been reported to promote point mutations of tumor cell generating neoantigens and cause tumor suppression (*5*). This xenogenization of tumor cells either increases their antigenicity or generates danger signals, which activate dendritic cells (DCs) to induce cross-presentation of tumor antigens to $CD8^+$ T cells.

Here, we demonstrate a new exosome-based approach for increasing the immunogenicity of tumors via xenogenization of tumor cells, triggering a robust antitumor immune response. Exosomes, which are membrane vesicles that shuttle genetic information and proteins between both neighboring and distant cells (*6*), are positioned to become a widespread tool for drug delivery (*7*, *8*). Exosomes can deliver membrane proteins into the right plasma membranes, which is an unresolved issue that scientists have wrestled with for more than a decade. To date, synthetic nanomaterials, including lipid vesicles, have been the mainstay delivery tool for protein drugs, but they cannot transfer the natural form of membrane proteins to the correct sites (*9*, *10*). Thus, exosomes are the only nanomaterials capable of transferring membrane proteins including transmembrane domain to the target cell membrane in their natural form, with maximized functionality (*11*). In our previous work, we developed a fusogenic exosome platform by performing exosome surface engineering with viral fusion proteins. We used vesicular stomatitis virus glycoprotein (VSV-G) that mediates membrane fusion at acidic pH. These virus-mimetic fusogenic exosomes were engineered to direct the transfer of active membrane proteins into target cell membranes (*12*).

To harness tumor cell xenogenization, we designed a recombinant fusogenic exosome harboring viral fusion–mediated glycoproteins (FMGs). These exosomes undergo membrane fusion with cancer cells, deliver FMGs to the recipient cancer cell membranes (membrane-editing), and modify the cancer cell membrane to present PAMPs that enable the immune system to recognize the cancer cells as non-self (i.e., by perceiving the "danger" signal).

Observations from several clinical studies of tumor immunology have indicated that exposure to PAMPs via vaccination or infection can have prophylactic and therapeutic effects on neoplastic diseases (*13*, *14*). For example, the attenuated live strain of *Mycobacterium bovis*, Bacille Calmette-Guérin (BCG), has now been approved by the U.S. Food and Drug Administration to treat nonmuscle invasive bladder cancer (*15*). Furthermore, the *Salmonella minnesota* lipopolysaccharide (LPS) variant monophosphoryl lipid A (MPL) is used as a prophylactic vaccine adjuvant for human papilloma virus (type 16 and 18)–related cervical cancer (*16*). Recently, oncolytic viruses were reported to boost antitumor T cell immune response through the PAMP-mediated cancer cell phagocytosis by DCs (*17*).

[1]KU-KIST Graduate School of Converging Science and Technology, Korea University, 145, Anam-ro, Seongbuk-gu, Seoul 02841, Republic of Korea. [2]Biomedical Research Institute, Korea Institute of Science and Technology (KIST), Seoul 02792, Republic of Korea. [3]Research Animal Resource Center, Korea Institute of Science and Technology (KIST), Seoul 02792, Republic of Korea. [4]Division of Bio-Medical Science &Technology, KIST School, Korea University of Science and Technology, Seoul 02792, Republic of Korea.
*These authors contributed equally to this work.
†Corresponding author. Email: iskim14@kist.re.kr (I.-S.K.); ysyang@kist.re.kr (Y.Y.)

PAMPs secreted from dying tumor cells, which are immunogenic, interact with various receptors of innate immune cells (*18*). The Toll-like receptors (TLRs), which consist of a family of pattern recognition receptors, can detect a plethora of PAMPs to trigger the activation and maturation of DCs through enhanced expression of costimulatory molecules.

Here, to introduce PAMPs onto cancer cell membranes, we used a mutant form of VSV-G that efficiently promotes membrane fusion at the tumor extracellular pH (*19*). The fusogenic exosome enables viral PAMPs to be efficiently transferred into the cancer cell membrane. These xenogenized tumor cells can be readily recognized and engulfed by DCs, thereby eliciting the anticancer immune responses. Combination therapy with anti–PD-L1 antibodies yielded potent tumor-specific immune responses. Together, our findings provide a rationale for the therapeutic application of exosome-based tumor xenogenization to enhance tumor immunogenicity and induce potent anticancer immunity.

RESULTS

Exosome-mediated xenogenization enhances cancer cell phagocytosis

VSV-G is a widely studied fusogenic membrane glycoprotein that mediates membrane fusion only at acidic pHs between 4.8 and 6.4. On the basis of a previous report that the pH selectivity of VSV-G toward tumor tissues (to pH 6.5 to 7.1) could be improved by introducing the point mutation H162R (*19*), we tested whether exosomes expressing this mutant VSV-G on their surfaces could fuse with cancer cells in the weakly acidic tumor microenvironment. Plasmids encoding mutant VSV-G H162R (mVSVG) were generated by site-directed mutagenesis and transfected into human embryonic kidney (HEK) 293T cells. After 48 hours, exosomes were collected by harvesting the conditioned medium and subjecting it to filtration and ultracentrifugation. As controls, media were collected from HEK293T cells subjected to transfection of mock plasmids (Con-Exo) or plasmids encoding wild-type VSV-G (wtVSVG-Exo) or CD63-GFP (GFP-Exo).

The engineered exosomes expressing VSV-G proteins on their membranes (mVSVG-Exo) were spherical in shape with a diameter of ~80 nm (Fig. 1, A and B). Other exosomes (wtVSVG-Exo, GFP-Exo, and Con-Exo) were confirmed to have similar properties to mVSVG-Exo, as indicated in our previous study (fig. S1A) (*12*). To determine whether mVSVG-Exo could fuse with cancer cell membranes to mediate delivery of VSV-G under in vitro conditions, we used confocal microscopy and flow cytometry to track the location of VSV-G proteins in the 4T1-Luc, EL4-Ova, and CT26.CL25 cancer cell lines. VSV-G requires low-density lipoprotein receptors (LDLRs) as fusion partners as well as low pH for mediating fusion. Fortunately, tumor lesions have areas of low pH (weakly acidic) (*20*) and express high level of LDLRs (fig. S1B) (*21*). Therefore, we took advantage of the pH-sensitive abilities and LDLR specificities of VSV-G for selective targeting of the tumor cells. Our results showed that, at pH 6.8, mutant VSV-G was transferred from the exosomes to 4T1-Luc cancer cell membranes at much higher levels than wild-type VSV-G (delivered by wtVSVG-Exo) (Fig. 1C and fig. S1, C and D). However, we observed no significant differences in exosome-mediated mVSVG delivery in BALB/3T3 fibroblasts, which hardly express LDLR proteins (fig. S1, E and F). In addition, treatment of 4T1-Luc cells with mVSVG-Exo caused a concentration-dependent increase in membrane editing at pH 6.8, whereas this was not seen in the other groups (fig. S2). Notably, exosome-mediated VSV-G delivery was observed for both wild-type and mutant proteins at pH 5.5 (Fig. 1C). Transfer of mutant VSV-G at pH 6.8 was also observed in EL4-Ova lymphoma cells and CT26.CL25 colon cancer cells (fig. S3A). After 12 hours, the VSV-G proteins transferred from mVSVG-Exo were hardly observed in 4T1-Luc cell membranes, where they stayed for at least 4 hours (fig. S3B). Collectively, these results demonstrate that mVSVG-Exo can efficiently deliver the mutant VSV-G proteins to the cancer cell surface under weakly acidic conditions.

VSV-G has been reported to be sensed by the innate immune cells as a PAMP (*22*). For this reason, mVSVG-Exo or wtVSVG-Exo treatment on bone marrow–derived macrophages (BMDMs) induced the release of proinflammatory cytokines [interleukin-6 (IL-6) and tumor necrosis factor–α (TNF-α)], chemokines (CXCL10/CRG-2 and CXCL1), and adhesion molecules (sICAM-1) to the extent similar with LPS treatment (fig. S4A). To verify that this viral PAMP can enhance the activity of phagocytes, we evaluated whether exosome-mediated mVSVG xenogenization increased the in vitro phagocytic activity of BMDMs and bone marrow–derived DCs (BMDCs) co-cultured with various tumor cell lines. Our result showed that cancer cells (EL4-Ova, 4T1-Luc, and CT26.CL25) fused with mVSVG-Exo and cultured at pH 6.8 were more readily engulfed by BMDMs and BMDCs compared with the relevant controls (Fig. 1D and figs. S4, B to D, and S5, A and B). This phagocytic activity of BMDMs and BMDCs was decreased by preblocking with anti–VSV-G antibodies, indicating that the effect was VSV-G dependent (Fig. 1D and fig. S4, C to E). To exclude the possibility that cancer cell death was induced by mVSVG-Exo–mediated membrane editing, we performed CCK-8 (Cell Counting Kit–8) assays after 24 hours of mVSVG-Exo treatment. As shown, exosome-mediated mVSVG delivery on 4T1-Luc and EL4-Ova cancer cells did not cause any significant change in cell viability (fig. S5, C and D).

Next, we assessed the antitumor effects of mVSVG-Exo in vivo using the EL4-Ova lymphoma syngeneic tumor model mice. After the tumor was around the size of 100 mm^3, mice were intratumorally administered with mVSVG-Exo, wtVSVG-Exo, or Con-Exo. As shown in Fig. 2A, mVSVG-Exo treatment significantly inhibited tumor growth, whereas treatment with wtVSVG-Exo only slowed tumor growth and Con-Exo and GFP-Exo had no impact on tumor progression (Fig. 2, A and B, and fig. S6A). There was no significant between-group difference in body weight (fig. S6B).

We also evaluated the antitumor ability of mVSVG-Exo against other tumors, using CT26.CL25-mCherry and 4T1-Luc orthotopic tumor models in mice. The results showed that mVSVG-Exo mediated successful tumor regression in both mouse models (Fig. 2, C and D, and fig. S6, C to E). Note that, as the 4T1-Luc breast tumor model is one of the most aggressive breast cancer cell lines, the in vivo antitumor effect of mVSVG-Exo on the 4T1-Luc tumor (fig. S6, C and D) was lower than that on either EL4-Ova or CT26.CL25-mCherry tumors (Fig. 2, A to D). To determine whether the mVSVG-Exo–induced antitumor activity was mediated by tumor cell xenogenization, we used flow cytometry to detect the retained VSV-G proteins on cancer cell membranes. Two hours after intratumoral administration of exosomes, tumor tissues were resected and dissociated to single cells, and the VSV-G proteins on cancer cell membranes were stained using an anti–VSV-G antibody. VSV-G proteins delivered by mVSVG-Exo were found on the surfaces of CT26.CL25-mCherry cancer cells. However, $VSV\text{-}G^+$ signals were hardly observed in other

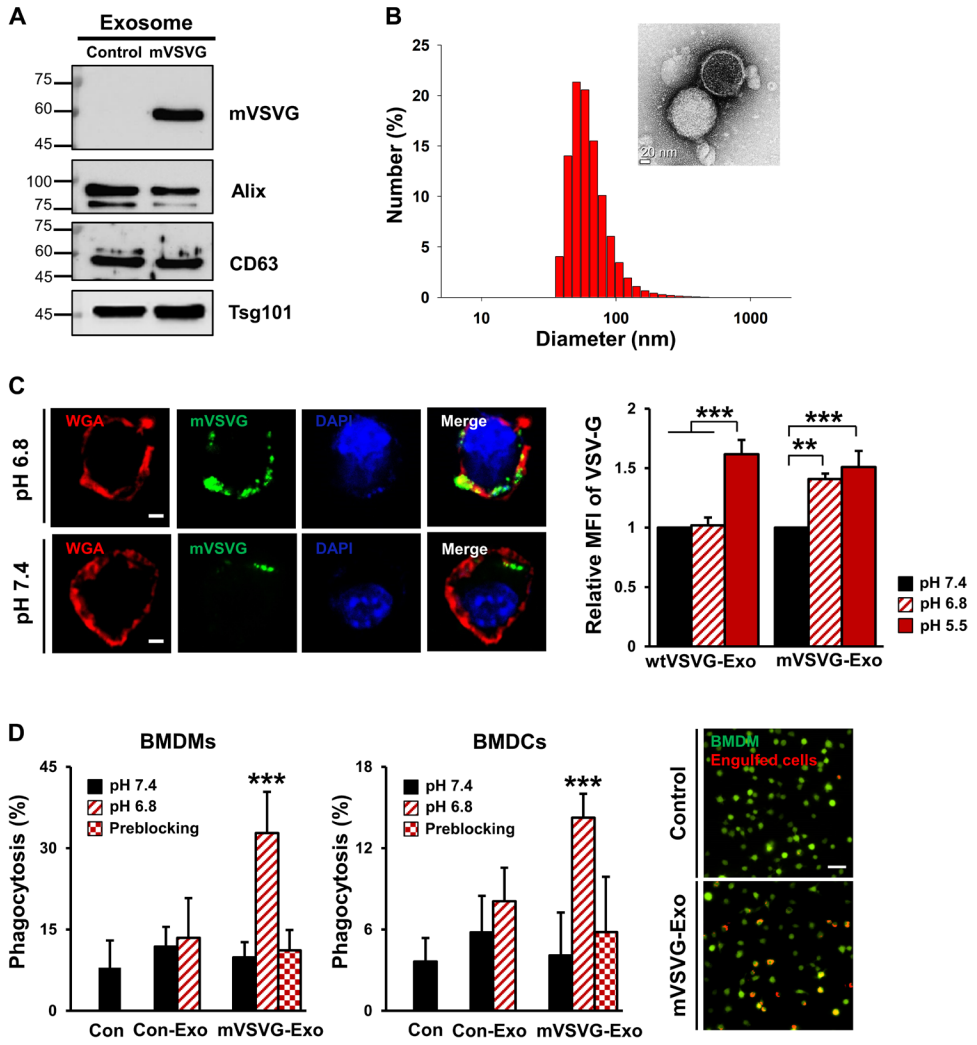

Fig. 1. mVSVG-Exo fuses with cancer cell membrane and enhances phagocytosis of cancer cells. (**A**) Western blotting of mVSVG-Exo and Con-Exo was performed to detect VSV-G and the exosomal markers Alix, CD63, and Tsg101. (**B**) Size distribution of mVSVG-Exo, as assessed using dynamic light scattering analysis. Inset image: Representative transmission electron microscopy (TEM) image of mVSVG-Exo. (**C**) Representative confocal immunofluorescence images (left) showing that mVSVG-Exo (green) fuses with 4T1-Luc cell membranes (red) at pH 6.8 (upper) but not at pH 7.4 (lower). The membrane-editing capacity of mVSVG-Exo and wtVSVG-Exo with 4T1-Luc cells under different pH conditions was quantified by flow cytometry (right). The total amount of exosomal protein treated in cancer cells was equalized by BCA protein assay. Data are presented as the relative MFI toward the pH 7.4 group ($n = 3$). WGA, wheat germ agglutinin; DAPI, 4′,6-diamidino-2-phenylindole. (**D**) pHrodo-labeled 4T1-Luc cells pretreated with exosomes were cocultured with 5-chloromethylfluorescein diacetate (CMFDA)–labeled BMDMs or BMDCs for 2 hours under the indicated conditions, and the percentages of phagocytosis were measured by counting the numbers of engulfed 4T1-Luc cells with BMDMs or BMDCs (left; $n = 6$ to 8). Representative microscopic pHrodo images of BMDMs against 4T1-Luc cells (right). Scale bars, 50 μm. *P* values were determined by one-way analysis of variance (ANOVA) with Tukey's post hoc test; $^{**}P < 0.01$, $^{***}P < 0.001$.

cell types ($CD45^+$ immune cells, $CD31^+$ endothelial cells, and $CD90.2^+$ cancer-associated fibroblasts) of the tumor microenvironment (Fig. 2, E and F, and fig. S7, A to C). Low LDLR expression was detected in these normal cells (fig. S7E). We also confirmed that there is no change in the pH of tumor tissues (pH ~6.8) before and after injection of pH 7.4 solutions (fig. S7D).

Because the CT26.CL25 cell expressing mCherry was initially generated to enable monitoring of in vivo phagocytosis (*23*), we were able to analyze the engulfment of CT26.CL25-mCherry cells by phagocytes (DCs and macrophages) in tumor tissues of the syngeneic tumor model. Our results showed that there were far more $mCherry^+$ macrophages and DCs in mVSVG-Exo–treated mice compared to control mice (Fig. 2, G and H, and fig. S8A). These results demonstrate that mVSVG-Exo–mediated xenogenization contributes to enhancing phagocytosis, which is an important part of eliciting an antitumor effect.

DC-mediated T cell priming is important for the antitumor immunity triggered by mVSVG-Exo

After DCs engulf a tumor cell, they process the tumor-derived antigens and then migrate toward a lymph node (LN) to undergo maturation. The matured DCs then prime effector T cells to activate the cancer-specific immune response (*24*). Here, we used flow cytometric analysis to evaluate the ability of DCs to present the captured antigens

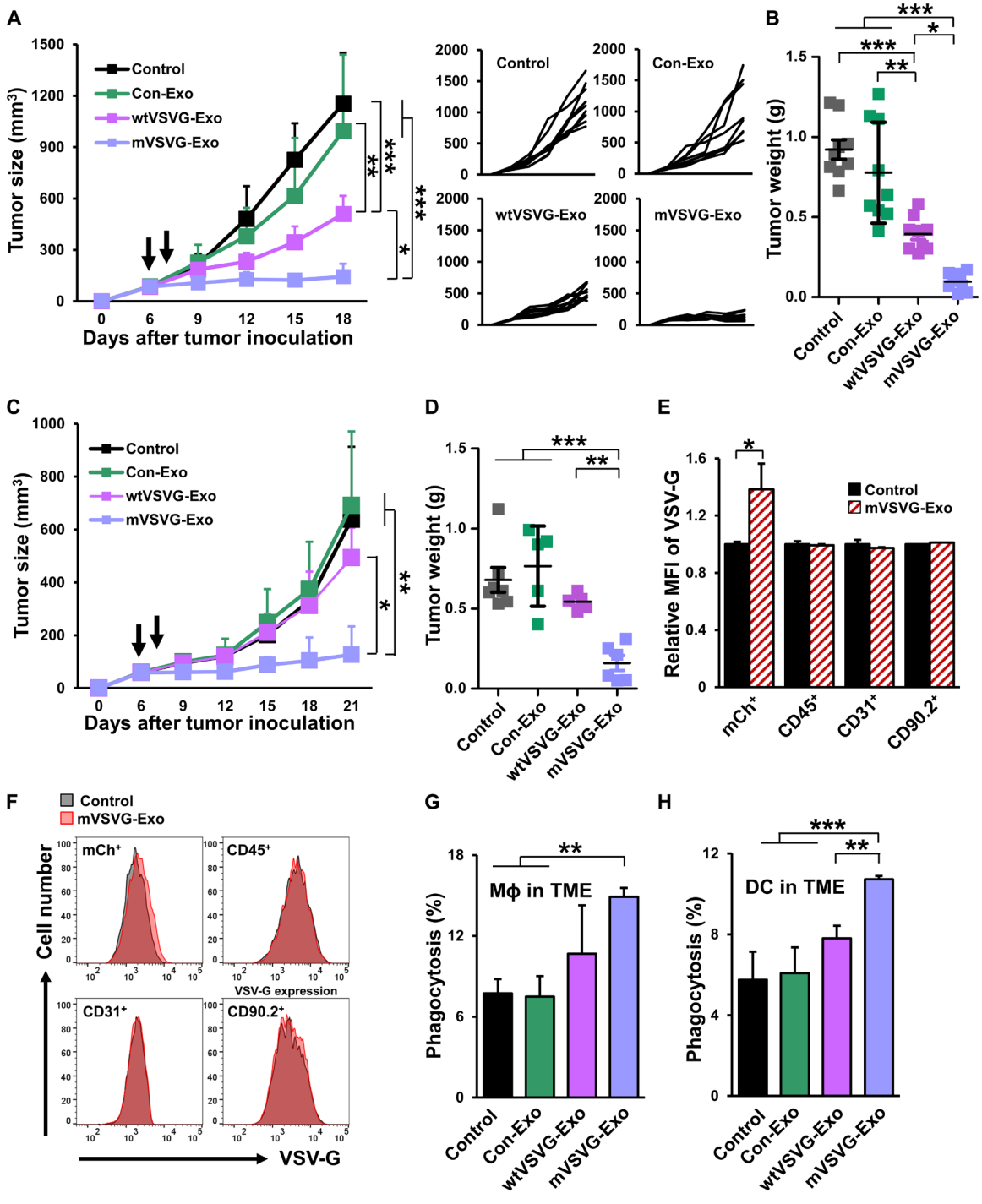

Fig. 2. mVSVG-Exo induces antitumor immunity. On day 6, EL4-Ova (**A** and **B**) or CT26.CL25-mCherry (**C**, **D**, **G**, and **H**) tumor models were treated (intratumorally) twice at a 1-day interval with 100 μg of mVSVG-Exo, wtVSVG-Exo, Con-Exo, or PBS. (A) Tumor size (mm^3) profiles ($n = 9$). (B) Tumor weight (g) at day 18 was analyzed ($n = 9$). (C) Tumor size (mm^3) profiles ($n = 5$ to 7). (D) Tumor weight (g) at day 21 was analyzed ($n = 5$ to 7). (**E**) When the average CT26.CL25-mCherry tumor volumes reached 100 mm^3, mice were treated (intratumorally) with 100 μg of mVSVG-Exo, wtVSVG-Exo, Con-Exo, or PBS. After 2 hours, tumors were collected and processed to single-cell suspensions. The level of VSV-G on sorted cells was assessed by flow cytometry. Data are presented as means of relative MFI toward the control ($n = 4$). (**F**) Representative histogram images of VSV-G signals from indicated cells. (G and H) Macrophages and DCs were isolated from tumors on day 10 after tumor inoculation. The percentage of macrophages or DCs containing $mCherry^+$ signals was determined by flow cytometry ($n = 4$). TME, tumor microenvironment. Arrows indicate treatment time points. *P* values were determined by one-way ANOVA with Tukey's post hoc test or Student's *t* test; $^*P < 0.05$, $^{**}P < 0.01$, $^{***}P < 0.001$.

to T cells in vivo. As shown in Fig. 3A, mVSVG-Exo markedly increased the cross-presentation of an Ova-specific antigen to major histocompatibility complex (MHC) class I by DCs ($CD11c^+$) in tumor-draining LNs of EL4-Ova tumor models. In contrast, the other tested exosomes did not affect the cross-presentation of Ova-derived peptides complexed with MHC-I on DCs (Fig. 3A and fig. S8B).

DC maturation can be triggered by the phagocytosis of dying tumor cells (*25*) and by TLR4 agonists (*26*). Because VSV-G has been

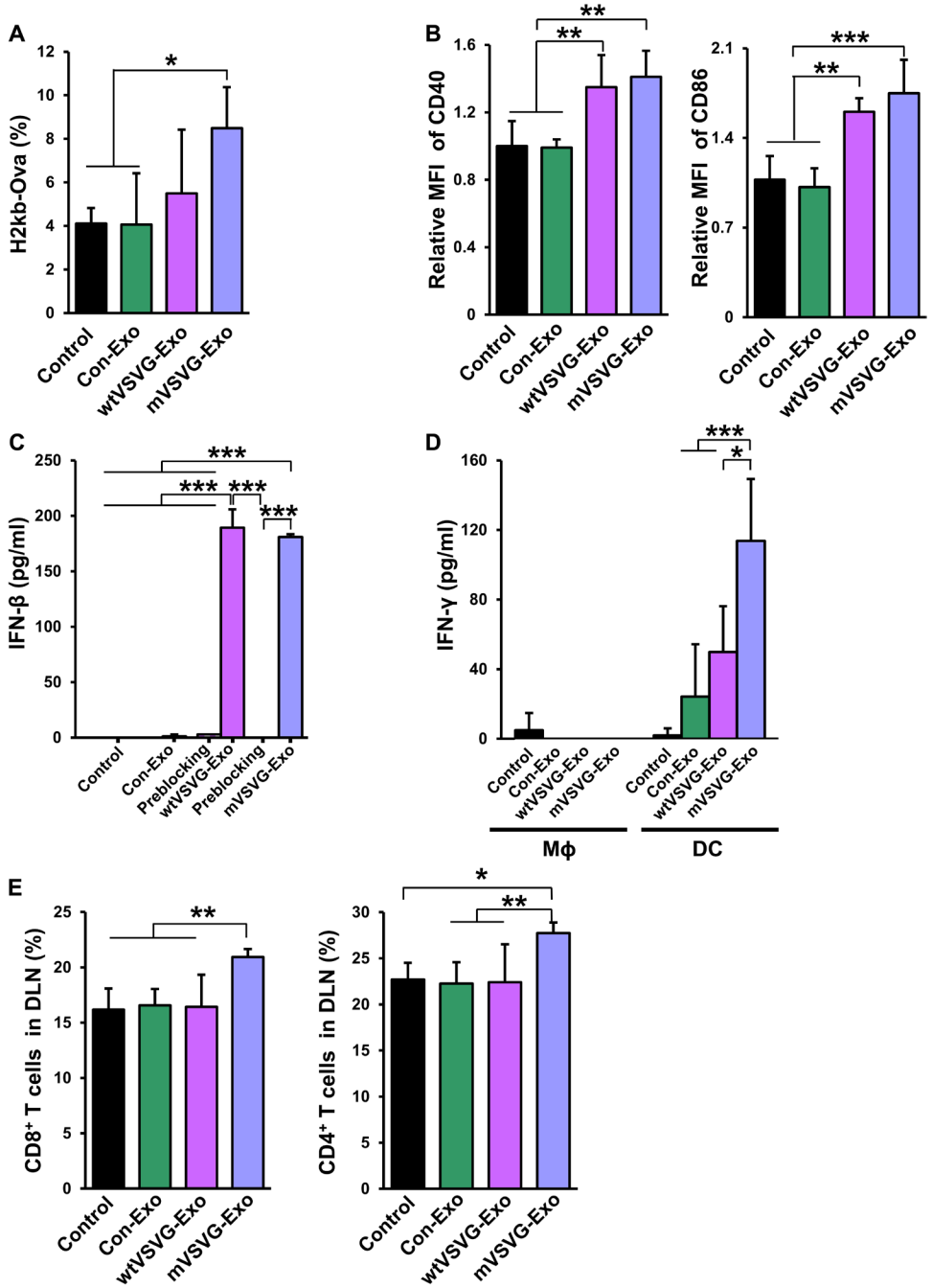

Fig. 3. Exosomes harboring VSV-G enhance TLR4-mediated DC cross-priming. (**A**, **B**, **D**, and **E**) On day 6 after tumor inoculation, EL4-Ova tumor models were treated (intratumorally) twice at a 1-day interval with 100 μg of mVSVG-Exo, wtVSVG-Exo, Con-Exo, or PBS. Tumor tissues or tumor-draining LN cells were extracted at day 18. (A) The percentage of H2kb-OVA^+ in $CD11c^+$ cells was analyzed by flow cytometric analysis ($n = 4$ or 5). (B) The average levels of CD40 or CD86 on DCs ($CD11c^+$ cells) were analyzed by flow cytometric analysis. Data are presented as the relative MFI toward the control ($n = 4$ or 5). (**C**) IFN-β production of BMDCs treated with 10 μg of mVSVG-Exo, wtVSVG-Exo, Con-Exo, or PBS was assessed by enzyme-linked immunosorbent assay (ELISA) ($n = 2$). (D) Macrophages ($F4/80^+$ cells) or DCs ($CD11c^+$ cells) of tumor tissues were cocultured for 72 hours with OT-I cells, and the amount of IFN-γ was assessed by ELISA ($n = 3$ to 5). (E) The percentage of $CD8^+$ T cells ($CD45.2^+CD3^+CD8^+$) and $CD4^+$ T cells ($CD45.2^+CD3^+CD4^+$) was evaluated by flow cytometric analysis in tumor-draining LN (DLN) ($n = 6$). *P* values were determined by one-way ANOVA with Tukey's post hoc test; $^*P < 0.05$, $^{**}P < 0.01$, $^{***}P < 0.001$.

found to act as a TLR4 agonist (*27*), we verified the effect of our exosomes on TLR4-mediated DC maturation. To assess in vivo DC maturation following exosome treatment, we detected the expression levels of costimulatory molecules (CD40 and CD86) on DCs in tumor-draining LNs of our EL4-Ova tumor model. The results showed that exosomes containing both wild-type and mutant VSV-G (wtVSVG-Exo and mVSVG-Exo) increased the expression levels of CD40 and CD86 on DCs from tumor-draining LNs (Fig. 3B and fig. S8, C and D). More in vivo DC maturation was associated with wtVSVG-Exo treatment, correlating with the slight decrease in tumor progression seen in wtVSVG-Exo–treated EL4-Ova tumor model mice (Fig. 2A).

Given that VSV-G can activate TLR4-mediated innate immunity (*28*), we further investigated whether exosomes containing VSV-G could induce type I interferon (IFN)–related responses in BMDCs. We found that both mVSVG-Exo and wtVSVG-Exo triggered a marked production of IFN-β, which is known to enhance the maturation and cross-priming capability of DCs. This increased production of IFN-β was abolished in cells that were preblocked with an anti-TLR4–neutralizing antibody (Fig. 3C).

As described above, mVSVG-Exo could enhance TLR4-mediated DC maturation, cancer cell phagocytosis, and antigen presentation. To investigate whether mVSVG-Exo treatment potentiates the capability of DCs to prime $CD8^+$ T cells, we analyzed ex vivo IFN-γ production by T cells that had been primed with DCs and macrophages from EL4-Ova tumor tissues in syngeneic mice. When tumor tissue–derived DCs were incubated with OVA-specific OT-I T cells, considerable increased IFN-γ production was measured in the mVSVG-Exo–treated group, whereas macrophages did not show increased T cell activation (Fig. 3D). Consistent with these results, mVSVG-Exo treatment significantly increased the frequency of $CD8^+$ T cells ($CD45.2^+CD3^+CD8^+$) and $CD4^+$ T cells ($CD45.2^+CD3^+CD4^+$) in tumor-draining LNs, in which T cells were educated by antigen-presenting cells (Fig. 3E and fig. S9, E and F). These results suggest that the cross-priming ability of DCs is important for augmenting an antitumor immune response after mVSVG-Exo treatment.

Therapeutic effect of mVSVG-Exo requires $CD8^+$ T cells

To determine the role of T cell immunity in the antitumor immune response triggered by mVSVG-Exo, we inoculated EL4-Ova cells into T cell–deficient nude mice. In contrast to the results presented in Fig. 2A, the same course of intratumoral mVSVG-Exo treatment that was effective in immunocompetent mice showed no tumor growth inhibition in immunodeficient nude mice (Fig. 4A and fig. S9A). However, when we doubled the dosing frequency, tumor growth was slightly inhibited even in immunodeficient nude mice (Fig. 4B and fig. S9B). These results were derived because "exosome-mediated xenogenization" can stimulate phagocytes such as DCs or macrophages to engulf some of the tumor cells. On the other hand, these results indicate that the mVSVG-Exo–mediated enhancement of phagocytosis is not sufficient for tumor growth inhibition and that T cell immunity appears to be required for the maximal therapeutic outcome. We further analyzed the effects of mVSVG-Exo on tumor growth in the EL4-Ova tumor model in $Batf3^{-/-}$ knockout (BATF3 KO) mice or mice depleted of $CD8^+$ T cells. BATF3 KO mice, which specifically lack $CD8^+$ and $CD103^+$ DCs, are unable to exhibit competent tumor-specific cytotoxic T cell immunity. Alternatively, $CD8^+$ T cells were depleted by intraperitoneal injection of a neutralizing antibody. Our results revealed that depletion of $CD103^+$ DCs or $CD8^+$ T cells robustly abrogated the antitumor response produced by mVSVG-Exo (Fig. 4, C and D, and fig. S9, C and D). These impaired antitumor effects suggest that mVSVG-Exo–mediated tumor regression is dependent on $CD8^+$ T cells.

We also performed immunofluorescence staining for $CD8^+$ cells in EL4-Ova tumor tissues to examine the local tumor-infiltrating $CD8^+$ T cells. We observed that mVSVG-Exo treatment significantly augmented an infiltration of $CD8^+$ T cells into tumors compared to that in the other groups (Fig. 4E and fig. S10, A and C). Notably, mVSVG-Exo treatment markedly activated the release of T helper 1 (T_H1) cytokines (IFN-γ, TNF-α, and IL-2) from $CD8^+$ T cells in EL4-Ova tumor tissues (Fig. 4F). Moreover, the number of MDSCs (Myeloid Derived Suppressor Cells) ($CD45.2^+CD11b^+GR\text{-}1^+$), which dampen antitumor immunity, was reduced in the tumor tissues (fig. S10, B and D). This changed immune contexture in tumor demonstrates that mVSVG-Exo can strongly elicit a local immune response in the tumor site, leading to the tumor regression by triggering systemic T cell immune responses.

Combination of mVSVG-Exo plus an anti–PD-L1 antibody effectively induces antitumor immunity

Programmed death ligand-1 (PD-L1) on tumor cells is often upregulated by IFN-γ production within the tumor microenvironment and is correlated with the response rate of PD-1/PD-L1 blockade (*29*, *30*). To assess whether mVSVG-Exo promotes the production of IFN-γ against tumor-specific antigens, we extracted splenocytes from EL4-Ova syngeneic tumor model mice and analyzed their immunological response against the Ova peptide. Splenocytes from mVSVG-Exo–treated mice produced more IFN-γ in response to the Ova peptide compared to the control mouse groups (Fig. 5A). As expected, mVSVG-Exo treatment also markedly increased IFN-γ–mediated PD-L1 expression in the tumor microenvironment (Fig. 5B).

Next, we examined the therapeutic effect of combination therapy using immune checkpoint blockade together with mVSVG-Exo in the EL4-Ova syngeneic tumor model. Anti–PD-L1 monotherapy had no impact on tumor progression, and monotherapy with mVSVG-Exo inhibited tumor growth but did not trigger complete tumor regression. In contrast, the combination treatment of mVSVG-Exo plus anti–PD-L1 yielded a marked tumor-suppressing effect, inducing complete tumor regression in 30% (3 of 10) of mice and improving overall survival (Fig. 5, C and D, and fig. S10E). To determine whether this combination therapy elicited tumor-specific immunologic memory, we selected mice found to be tumor-free after combined therapy and re-injected them with EL4-Ova tumor cells. While EL4-Ova tumor cell rechallenge resulted in rapid tumor growth in naive mice, mice that had eliminated the primary tumor after combined therapy were entirely resistant to rechallenge with same tumor cells (Fig. 5E). Collectively, these results indicate that combination therapy with mVSVG-Exo plus anti–PD-L1 contributes to inducing a specific and long-lasting systemic immune memory response that can eradicate the primary tumor and prevent recurrence.

DISCUSSION

On the basis of our previous study using engineered exosomes to direct transfer of functional membrane proteins into cellular membranes (*12*), here we used fusogenic exosomes that harbor mutant VSV-G working at pH 6.8, thereby delivering viral PAMPs to the cancer cell membranes. This novel exosome-based xenogenization method can increase the probability of tumor cells to be recognized

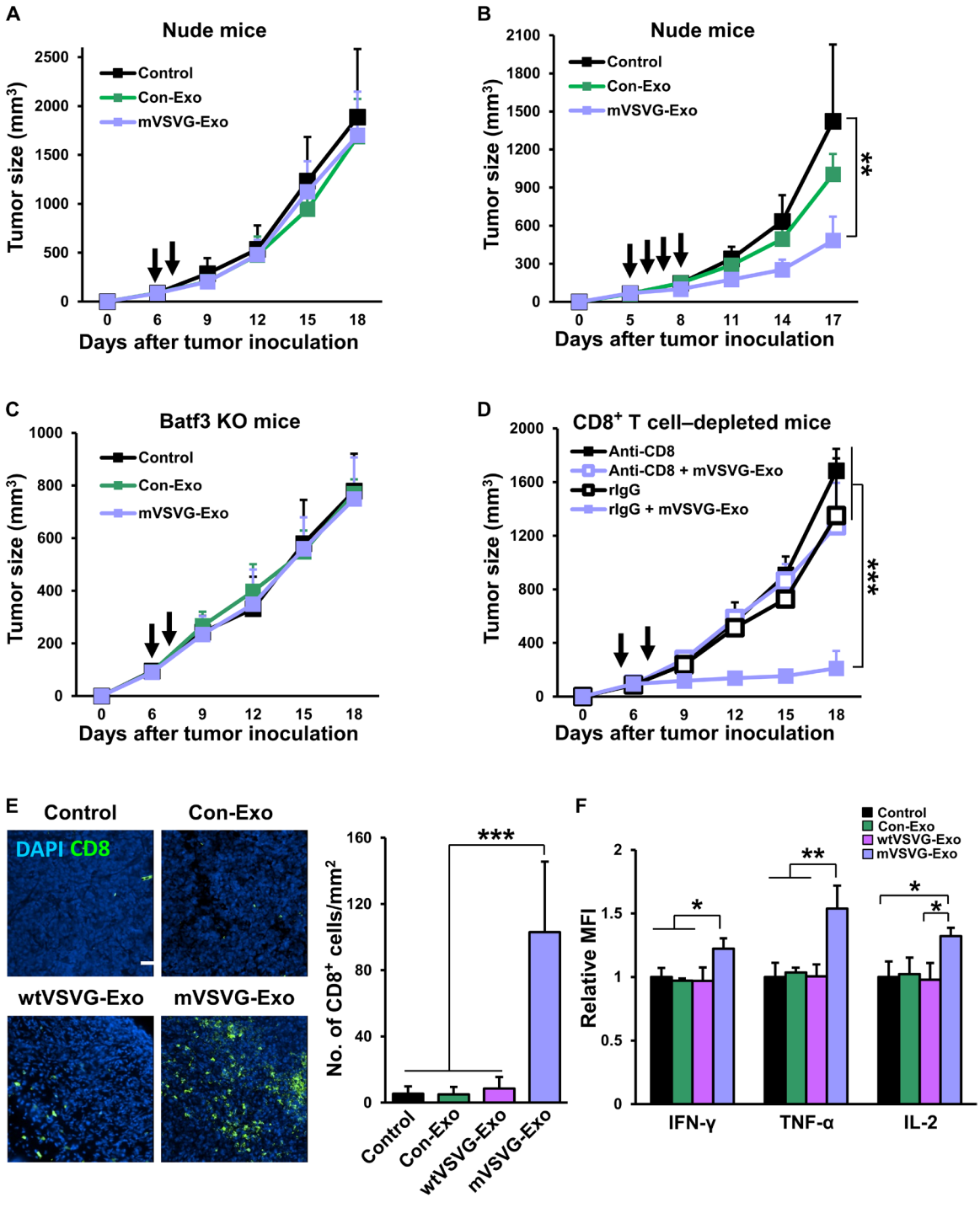

Fig. 4. Antitumor effect of mVSVG-Exo requires CD8$^+$ T cell immunity. (**A**) EL4-Ova tumor-bearing nude mice, (**C**) Batf3 KO mice, or (**D**) CD8$^+$-depleted mice were injected (intratumorally) twice with 100 μg of mVSVG-Exo, Con-Exo, or PBS. Tumor size (mm^3) profiles ($n = 5$ to 6). (**B**) EL4-Ova tumor-bearing nude mice were treated (intratumorally) four times with 100 μg of mVSVG-Exo, Con-Exo, or PBS. Tumor size (mm^3) profiles ($n = 6$ to 8). Arrows indicate treatment time points. (**E** and **F**) On day 6 after tumor inoculation, EL4-Ova tumor-bearing mice were treated (intratumorally) twice at a 1-day interval with 100 μg of mVSVG-Exo, wtVSVG-Exo, Con-Exo, or PBS. Tumor tissues of EL4-Ova tumor models were extracted at day 18. (E) Representative immunofluorescence images (left) of CD8$^+$ T cell infiltration in the tumor tissues from treated mouse. The number of CD8$^+$ T cells per mm^2 was analyzed using ImageJ software (right) ($n = 10$ to 12). Scale bars, 50 μm. (F) The average levels of IFN-γ, TNF-α, or IL-2 on CD8$^+$ T cells in tumor tissues were evaluated by flow cytometry. Data are presented as means of relative MFI toward the control ($n = 3$). *P* values were determined by one-way ANOVA with Tukey's post hoc test; *$P < 0.05$, **$P < 0.01$, ***$P < 0.001$.

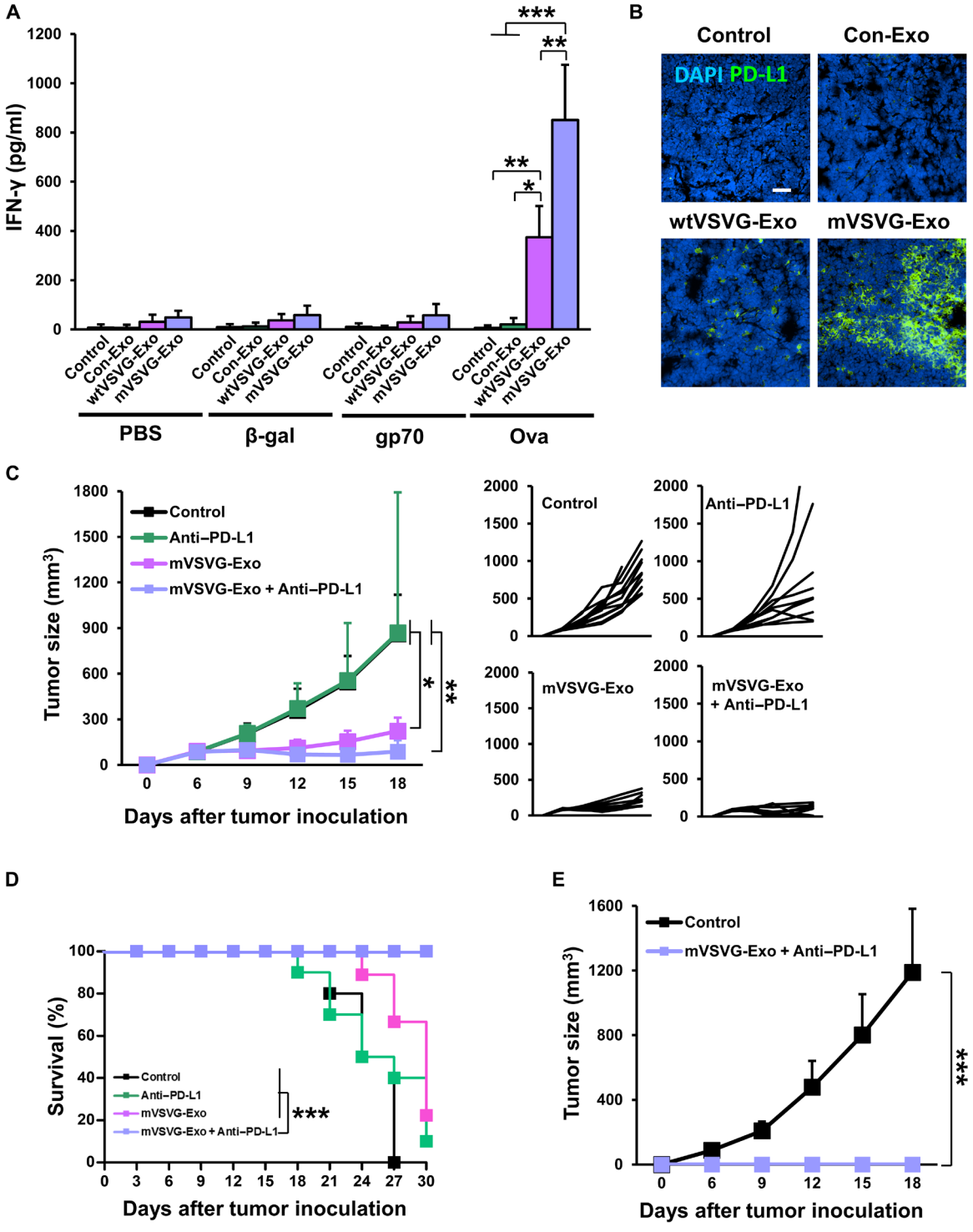

Fig. 5. Combined treatment with mVSVG-Exo plus anti–PD-L1 effectively induces antitumor immunity. (**A** and **B**) On day 6 after tumor inoculation, EL4-Ova tumor models were treated (intratumorally) twice at a 1-day interval with 100 μg of mVSVG-Exo, wtVSVG-Exo, Con-Exo, or PBS. Splenocytes and tumor tissues of EL4-Ova tumor models were extracted at day 10. (A) Splenocytes were stimulated with the Ova peptide, β-gal peptide, or gp70 peptide for 24 hours, and the amount of IFN-γ was evaluated by ELISA ($n = 3$ to 5). (B) Representative immunofluorescence images of tumor tissues stained with anti–PD-L1. (**C** to **E**) EL4-Ova tumor-bearing mice were treated with mVSVG-Exo (100 μg, intratumorally) on days 6 and 7, combined with PD-L1 antibody (200 μg, intraperitoneally) on days 10, 12, 14, and 16. (C) Tumor size (mm^3) profiles ($n = 10$). (D) Kaplan-Meier survival graphs of EL4-Ova tumor-bearing mice following the combination therapy ($n = 10$). (E) Tumor-free mice obtained after the combination therapy ($n = 3$) were rechallenged in the contralateral flank with 1×10^6 EL4-Ova cells at 1 month after their complete regression of the primary tumor. Scale bars, 50 μm. *P* values were determined by (A, C, and E) one-way ANOVA with Tukey's post hoc test and (D) the log-rank test; $^*P < 0.05$ $^{**}P < 0.01$, $^{***}P < 0.001$.

by DCs and renders immunologically cold tumors to T cell–inflamed (hot) tumors (Fig. 6). First, we found that fusogenic exosomes could deliver mVSV-G, a "viral antigen," to tumor cells selectively and xenogenized tumor cells promoted the phagocytic function of macrophage and DC in vitro and in vivo. The activation of phagocytes led to the enhanced presentation of tumor antigens to T lymphocytes. Second, exosome harboring mVSV-G induced TLR4-mediated DC maturation. In addition, we showed that the enhanced maturation and antigen-presenting activity of DCs increased $CD8^+$ T cell cross-priming. Third, the administration of these exosomes to mice representing multiple tumor models rendered the tumor cells more immunogenic, leading to decreased tumor growth. The therapeutic effect of mVSVG-Exo was dependent on $CD8^+$ T cell immunity. Furthermore, we suggested a therapeutic strategy combining mVSVG-Exo with anti–PD-L1 antibody that could augment antitumor immune responses, including complete tumor regression, better long-term survival, and conferred protection from tumor rechallenge.

Accumulating evidence indicates that the response rate of cancer immunotherapy is often associated with the immunogenicity of a tumor, with tumors bearing high mutational burden showing more improved response to immune checkpoint inhibitor than tumors bearing low mutational burden (*2*). We used our fusogenic exosome to deliver FMGs that modified cancer cell membranes to include PAMPs, which enabled the host immune system to recognize the tumor as foreign. As many tumors with low mutational burdens have the little inherent potential to elicit antitumor immune responses, our approach may prove to be a useful means to facilitate tumor immunogenicity by exposing PAMPs and to allow multiple types of cancer to respond to immune checkpoint blockades.

The idea of "xenogenization (or heterogenization)" was first defined in 1969 from the finding of the immunological rejection of transplanted tumors after artificial infection of tumors with murine leukemia viruses. These virus-infected tumors underwent regression because they had acquired a highly antigenic virus-specific antigen (*4*). These antigens were recognized as foreign to the host and thus precipitated a robust immune response against the tumor. Using viral xenogenization as a springboard, researchers next investigated chemical xenogenization. For example, the antitumor drug dacarbazine [dimethyltriazene-imidazole-4-carboxamide (DTIC)] was used to transplant antigens to malignant cells in leukemia-bearing mice (*5*, *31*). However, these strategies for viral and chemical tumor xenogenization failed to gain a toehold in the context of anticancer therapy. In an effort to develop a xenogenization, we demonstrated a simple exosome-based strategy that enabled a foreign antigen to be directly introduced onto the cancer cell membrane. Here, we used fusogenic exosomes to xenogenize tumor cells with a viral PAMP

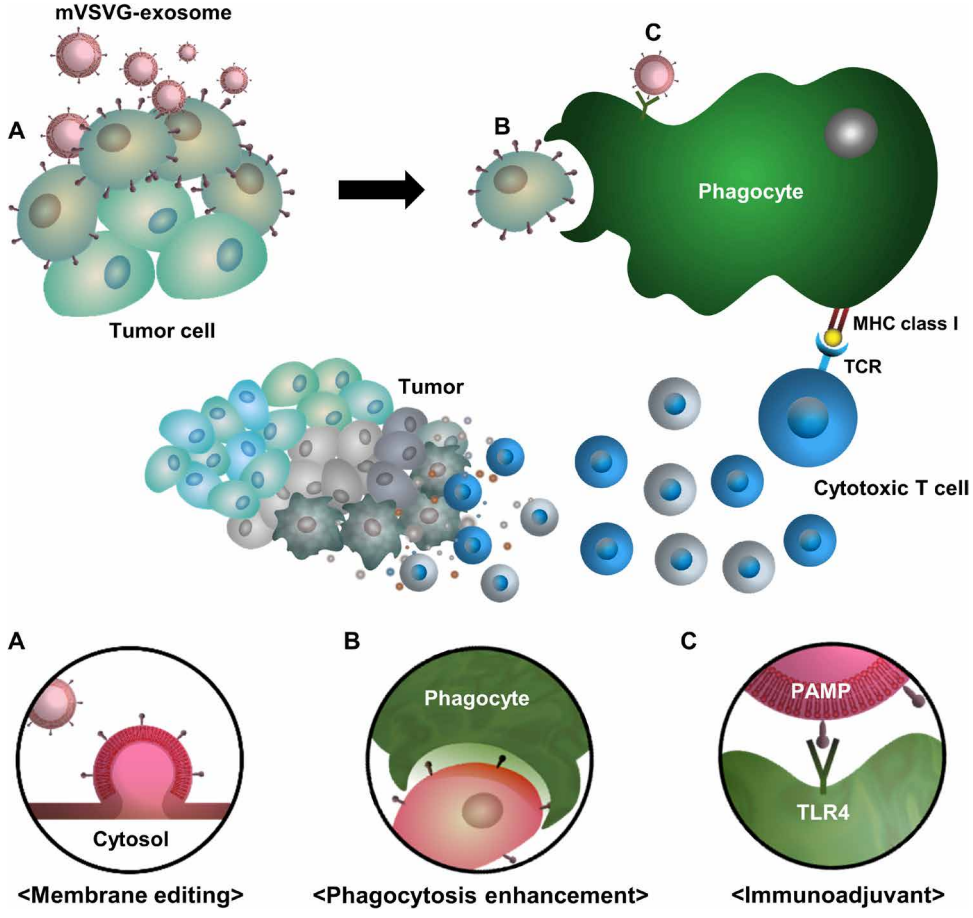

Fig. 6. Schematic illustration of mVSVG-Exo–mediated tumor xenogenization strategy. (**A**) mVSVG-Exo fuses with the tumor cell membrane in an LDLR- and pH-dependent manner. (**B**) mVSVG-edited tumor cells are more easily engulfed by phagocytes. (**C**) mVSVG-Exo can activate DC functions by stimulating TLR4 signaling. This strategy enhances cross-prime ability, which can further increase $CD8^+$ T cell immunity against cancer.

that is foreign to the host, leading to tumor regression. Our results highlight the potential immunotherapeutic anticancer use of exosomes hitherto unknown and revive the concept of enhancing tumor immunogenicity.

To translate this approach to the clinical application in cancer immunotherapy, many things are required to be solved (*11*). There are still challenges pertaining to the efficiency of protein delivery by fusogenic exosomes. The heterogeneity of exosomes makes it difficult to quantify and control the dose of PAMP proteins needed to enhance phagocytosis. Nevertheless, our present results indicate that exosome-induced xenogenization appears to offer a new approach for improving the therapeutic efficacy of immune checkpoint blockade in cancer patients. The proposed approach is expected to represent a powerful tool for understanding the direct communication between tumor immunogenicity and the cancer susceptibility to the host's immune responses.

MATERIALS AND METHODS

Animals

BALB/c, BALB/c nude, and C57BL/6 mice (age, 8 weeks) were purchased from Orient Bio. C57BL/6-Tg(TcraTcrb)1100Mjb/J and B6.129S(C)-Batf3tm1Kmm/J mice were purchased from The Jackson Laboratory. All mice were maintained and raised in a specific pathogen–free animal room at the Korea Institute of Science and Technology (KIST). All animal experiments were performed in accordance with the guidelines of the Institutional Animal Care and Use Committee (IACUC) of KIST.

Reagents

The neutralizing CD8 (clone: 2.43), isotype-matched control (clone: LTF-2), and PD-L1 antibodies (clone: 10F.9G2) were obtained from Bio X Cell. The CD86 [clone: GL-1, fluorescent: phycoerythrin (PE)], CD40 (clone: 3-23, fluorescent: PE), CD3 [clone: 17A2, fluorescent: fluorescein isothiocyanate (FITC)], CD8α [clone: 53-6.7, fluorescent: allophycocyanin (APC)], CD4 (clone: GK1.5, fluorescent: APC), IFN-γ (clone: XMG1.2, fluorescent: PE), TNF-α (clone: MP6-XT22, fluorescent: PE), IL-2 (clone: JES6-5H4, fluorescent: PE), CD11c (clone: N418, fluorescent: APC), F4/80 (clone: BM8, fluorescent: APC), CD274 (B7-H1, PD-L1) (clone: 10F.9G2, fluorescent: APC), CD45.2 (clone: 104, fluorescent: PE/Cy7), CD11b (clone: M1/70, fluorescent: FITC and APC), and Gr-1 (clone: RB6-8C5, fluorescent: FITC) antibodies were purchased from BioLegend. The rat immunoglobulin G1 (IgG1) isotype control antibody (clone: RTK2071, fluorescent: PE), rat IgG2a isotype control antibody (clone: RTK2758, fluorescent: APC, and PE), rat IgG2b (clone: RTK4530, fluorescent: APC, PE, and FITC), Armenian hamster IgG isotype control antibody (clone: HTK888, fluorescent: APC), and mouse IgG2a isotype control antibody (clone: MOPC-173, fluorescent: PE/Cy7) served as isotype-matched controls and were purchased from BioLegend. The CD8α (clone: 53-6.7), PD-L1 (clone: 10F.9G2), and rat IgG2a isotype control antibodies (clone: R35-95) were obtained from BD Pharmingen. The VSV-G (clone: P5D4), CD63 (clone: MEM-259), Tsg101 (clone: 4A10), green fluorescent protein (GFP) [ab 290, chromatin immunoprecipitation (ChIP) grade], and LDLR antibodies (clone: EP1553Y) were purchased from Abcam. Alix (clone: H270) and CD81 (clone: sc-166029) were obtained from Santa Cruz Biotechnology. The recombinant mouse macrophage colony-stimulating factor (M-CSF) and Flt-3 ligand protein were obtained from PeproTech. The $CD8^+$ T cell enrichment columns and IFN-γ and IFN-β enzyme-linked immunosorbent assay (ELISA) kits were purchased from R&D Systems. The 5-chloromethylfluorescein diacetate (CMFDA) and TLR4 (clone: MTS510) antibodies were obtained from Thermo Fisher Scientific. pHrodo-SE was obtained from Invitrogen. The CD90.2, CD31, CD45, F4/80, and CD11c microbeads and the Dead Cell Removal Kit were purchased from Miltenyi Biotec.

Cell culture

HEK293T and EL4-Ova lymphoma cells (gifted by S.-H. Lee; Korea Advanced Institute of Science and Technology, Republic of Korea) were cultured in Dulbecco's modified Eagle's medium high glucose (DMEM-high glucose, HyClone) with 10% fetal bovine serum (FBS; Gibco) and 1% antibiotics-antimycotics (Gibco). Murine 4T1-Luc breast tumor and CT26.CL25 colon tumor cells were maintained in RPMI 1640 (Welgene) containing 10% FBS (Gibco) and 1% antibiotic-antimycotics (Gibco). For differentiation into BMDMs, bone marrow cells separated from BALB/c or C57BL/6 mice were incubated with mouse M-CSF (20 ng ml^{-1}) (PeproTech) for 7 days. BMDCs were differentiated from bone marrow cells of C57BL/6 or BALB/c mice with Flt-3 ligand (PeproTech, 200 ng ml^{-1}) and 0.1% β-mercaptoethanol for 10 days. Flow cytometric analysis was performed to confirm the differentiation of BMDMs or BMDCs using F4/80 or CD11c antibody. OT-I cells were isolated from C57BL/6-Tg(TcraTcrb)1100Mjb/J mice using a $CD8^+$ T cell enrichment column. The CT26.CL25-mCherry cell line was developed by transduction of CT26.CL25 cells with mCherry-encoding retrovirus systems. mCherry expression was confirmed by flow cytometric analysis. Incubation conditions of all cells: 5% CO_2, 37°C. No mycoplasma contamination was detected in any cell line used in this study.

Characterization of purified mVSVG-exosome

Following medium change with serum-free DMEM-high glucose [supplemented with Glutamax (1%; Gibco) and antibiotics-antimycotics (1%; Gibco)], HEK293T cells were subjected to DNA transfection. Transfection was performed with plasmid encoding mVSVG (20 μg) and Lipofectamine 3000 (Invitrogen). After 48 hours, supernatants were harvested. Cellular debris and microvesicles were removed by serial centrifugation (10 min at 300*g*, 10 min at 2000*g*, and 30 min at 10,000*g*). The supernatants were filtered with a 0.22-μm pore filter and ultracentrifuged for 3 hours at 150,000*g* in a 45 Ti rotor (Beckman Instruments). The obtained exosomal pellet was resuspended in phosphate-buffered saline (PBS) with proteinase inhibitors (Roche). The BCA Protein Assay Kit (Bio-Rad) was used for quantifying the total protein concentration of exosomes.

Dynamic light scattering

The size distribution of exosomes was analyzed by dynamic light scattering (DLS) using Zetasizer Nano ZS (Malvern Instrument, United Kingdom) with the following parameters: fixed angle, 173°; temperature, 25°C; and refractive index, 1.450. The measured data were analyzed using the program provided by the instrument.

Transmission electron microscopy

The structures of prepared exosomes were detected by transmission electron microscopy (TEM) (Tecnai System). In brief, exosomes (20 μg) fixed with 4% formaldehyde were placed on formvar/carbon-coated grids, washed with filtered PBS, and stained with uranyl acetate solution. After 24 hours of incubation, samples were analyzed with TEM.

Immunoblotting

The BCA protein assay was used for ensuring that equal concentrations of exosomes were prepared for SDS–polyacrylamide gel electrophoresis (SDS-PAGE). After SDS-PAGE, samples were transferred to nitrocellulose membranes. The blots were incubated overnight at 4°C with the following primary antibodies: VSV-G (clone: P5D4), Alix (clone: H270), CD63 (clone: MEM-259), Tsg101 (clone: 4A10), CD81 (clone: sc-166029), GFP (ab 290, ChIP grade), and LDLR (clone: EP1553Y). Next, the membranes were probed with horseradish peroxidase–conjugated anti-rabbit (Sigma-Aldrich) or mouse secondary antibody (Sigma-Aldrich). Last, the blots were visualized with enhanced chemiluminescence reagents (Bio-Rad).

Membrane-editing assays with mVSVG-Exo

To confirm the membrane-editing capacity of mVSVG-Exo, 5×10^5 4T1-Luc breast tumor cells, EL4-Ova lymphoma cells, or CT26.CL25 colon tumor cells were maintained for 10 min at 37°C with 50 μg of mVSVG-Exo, wtVSVG-Exo, or Con-Exo in 1 ml of fusion buffer (1.8 mM NaH_2PO_4, 10 mM Hepes, 8.4 mM Na_2HPO_4, 2.5 mM NaCl, 10 mM MES, with the pH adjusted with HCl to 5.5, 6.8, or 7.4). The cells were then washed and incubated with fresh medium for 1 hour. For our in vitro flow cytometry–based membrane-editing assay, 5×10^5 4T1-Luc breast tumor, EL4-Ova lymphoma, or CT26.CL25 colon tumor cells were incubated with 25, 50, or 100 μg of mVSVG-Exo, wtVSVG-Exo, or Con-Exo in with fusion buffer (pH 5.5, 6.8, or 7.4) for 10 min at 37°C and then incubated with fresh medium for 1 hour. Thereafter, the cells were stained with the VSV-G (clone: P5D4) antibody and then Alexa Fluor 647–conjugated secondary antibody (Jackson ImmunoResearch). For confocal analysis of the mVSVG-Exo–mediated transfer of mVSVG, 5×10^5 4T1-Luc breast tumor cells were incubated with mVSVG-Exo (50 μg) in fusion buffer (1 ml) at 37°C for 10 min. The cells were then seeded in a four-well chamber (154526, Nunc) with complete RPMI medium and incubated for 1, 4, 8, 12, or 16 hours. The cells were fixed with 4% paraformaldehyde (Biosesang), preblocked with 3% bovine serum albumin (BSA) solution (Affymetrix), and incubated with the VSV-G antibody (clone: P5D4) and then Alexa Fluor 488–conjugated secondary antibody (Jackson ImmunoResearch) with 1% BSA solution. The plasma membranes were labeled with wheat germ agglutinin (5 μg ml^{-1}) and Alexa Fluor 633 conjugate dye (Thermo Fisher Scientific) with 1% BSA solution. For our in vivo flow cytometry–based membrane-editing assay, BALB/c mice were implanted in the left flank with 1×10^6 CT26.CL25-mCherry cells. After the tumor reached an average size of 100 mm^3, mVSVG-Exo (100 μg), wtVSVG-Exo (100 μg), Con-Exo (100 μg), or PBS was administered via intratumoral injection. After 2 hours, tumors were isolated. Single tumor cell suspensions were generated using the MACS Tumor Dissociation Kit and the Dead Cell Removal Kit. The endothelial cells, cancer-associated fibroblasts, and immune cells were isolated using CD90.2, CD31, and CD45 microbeads (Miltenyi Biotec), respectively. Each of the isolated cells, including tumor cells, was incubated with the VSV-G (clone: P5D4) and Alexa Fluor 647–conjugated secondary antibodies (Jackson ImmunoResearch).

Proteome profiler mouse cytokine array

BMDMs (3.5×10^6 cells) were seeded in 90-mm petri dishes and pretreated with mVSVG-Exo (10 μg ml^{-1}), wtVSVG-Exo (10 μg ml^{-1}), GFP-Exo (10 μg ml^{-1}), and LPS (100 ng ml^{-1}) for 24 hours. After removing the particulates by centrifugation, 1 ml of the supernatant was used for cytokine detection using the Proteome Profiler Mouse Cytokine Array Kit (ARY006, R&D Systems).

Phagocytosis assay

For our in vitro phagocytosis assay, 2×10^5 BMDMs or BMDCs stained by 1 μM CellTracker Green CMFDA (Thermo Fisher Scientific) were seeded at the 35-mm dish. The following day, 4T1-Luc, EL4-Ova, or CT26.CL25 cells were labeled with pHrodo-SE (Thermo Fisher Scientific) and then cell membranes were fused with mVSVG-Exo, Con-Exo, or GFP-Exo under different pH conditions. To preblock VSV-G proteins on tumor cell surfaces, 10 μg of the anti–VSV-G antibody (clone: P5D4) was treated to 5×10^5 xenogenized tumor cells in FBS-free media (1 ml) at 4°C for 30 min. The mouse IgG1 monoclonal antibody (clone: 15-6E10A7) was used as a control antibody. The cells were then incubated with Green CMFDA–stained BMDMs or BMDCs at 37°C for 2 hours, and the signals of non-engulfed pHrodo-labeled cancer cells were removed with pH 10 of basic PBS. The phagocytosis of cancer cells was determined from six or more randomly chosen fields per assay analyzed with a fluorescence microscope (Nikon). For the in vivo phagocytosis assay, C57BL/6 mice were implanted in the left flank with 1×10^6 CT26.CL25-mCherry cells. After the average tumor size reached around 100 mm^3, mVSVG-Exo (100 μg), wtVSVG-Exo (100 μg), Con-Exo (100 μg), or PBS was administered twice at an interval of 1 day via intratumoral injection. At 72 hours after the second injection, extracted tumor tissues were enzymatically dissociated into single-cell suspensions with a tumor dissociation kit (Miltenyi Biotec). F4/80- and CD11c-specific magnetic beads (MACS isolation systems) were used to isolate macrophages ($F4/80^+$) and DCs ($CD11c^+$) from single tumor cell suspensions, and the populations of $mCherry^+$ DCs ($CD11c^+$) and macrophages ($F4/80^+$) were determined by flow cytometric analysis.

In vivo tumor models

BALB/c, BALB/c nude, or C57BL/6 mice have been used for syngeneic tumor models. Mice were implanted in the left flank with 1×10^6 4T1-Luc, EL4-Ova, or CT26.CL25-mCherry cells. When the average tumor size reached 70 to 120 mm^3 on day 6 following inoculation, mVSVG-Exo (100 μg), wtVSVG-Exo (100 μg), Con-Exo (100 μg), GFP-Exo (100 μg), or PBS was injected (intratumorally) twice at a 1-day interval. Tumor size was evaluated with calipers every 3 days and calculated as ($width^2 \times length$)/2. In some experiments, nude mice were implanted in the left flank with 1×10^6 EL4-Ova cells and injected intratumorally on days 5, 6, 7, and 8 after tumor inoculation with mVSVG-Exo (100 μg), Con-Exo (100 μg), or PBS. In other experiments, Batf3 KO mice (B6.129S(C)-Batf3tm1Kmm/J) were implanted in the left flank with 1×10^6 EL4-Ova cells and then injected intratumorally on days 6 and 7 after tumor inoculation with mVSVG-Exo (100 μg), Con-Exo (100 μg), or PBS. The tumor-bearing mice of EL4-Ova were treated with mVSVG-Exo (100 μg, intratumorally) on days 6 and 7 and then with PD-L1 antibody (clone: 10F.9G2, 200 μg, intraperitoneally) on days 10, 12, 14, and 16 for combination therapy. For the depletion of $CD8^+$ T cell in mice, neutralizing CD8 antibody (clone: 2.43, 200 μg, intraperitoneally) was treated on day 5 after tumor inoculation and every 3 days thereafter. Rat IgG2b (clone: LTF-2) was used as a control antibody. $CD8^+$ T cell depletion was confirmed by flow cytometric analysis with CD8α (clone: 53-6.7, fluorescent: APC) or rat IgG2a isotype control antibody (clone: RTK2758, fluorescent: APC).

Analysis of cross-presentation

For evaluating the degree of cross-presentation, the expression level of MHC-I molecule Kb (H2kb) bound to the Ova peptide (SIINFEKL) on DCs was observed by flow cytometry. The tumor-bearing mice of EL4-Ova were intratumorally injected with mVSVG-Exo (100 μg), Con-Exo (100 μg), wtVSVG-Exo (100 μg), or PBS on days 6 and 7 after tumor inoculation. On day 18, the tumor-draining LNs isolated from each mouse were mechanically dissociated into single-cell suspensions. The percentage of H2kb-OVA$^+$ in CD11c$^+$ DCs of tumor-draining LNs cells was analyzed by flow cytometric analysis using CD11c (clone: N418, fluorescent: APC) and H2kb-OVA (clone: 25-D1.16, fluorescent: PE) antibodies. IgG1 isotope (clone: MOPC-21, fluorescent: PE) and Armenian hamster IgG isotype antibody (clone: HTK888, fluorescent: APC) served as controls.

Analysis of DC maturation

For in vivo DC maturation analysis, the tumor-bearing mice of EL4-Ova were intratumorally injected with mVSVG-Exo (100 μg), Con-Exo (100 μg), wtVSVG-Exo (100 μg), or PBS on days 6 and 7 after tumor inoculation. On day 18, the tumor-draining LNs isolated from each mouse were mechanically dissociated into single-cell suspensions. The relative MFI (Mean Fluorescence Intensity) (relative to control) of CD86 or CD40 on CD11c$^+$ DCs of the tumor-draining LNs cells was analyzed by flow cytometry using CD11c (clone: N418, fluorescent: APC) plus CD40 (clone: 3-23, fluorescent: PE) or CD86 antibody (clone GL-1, fluorescent: PE). Rat IgG2a isotope (clone: RTK2758, fluorescent: PE) and Armenian hamster IgG isotype antibody (clone: HTK888, fluorescent: APC) served as controls.

Analysis of priming ability of DC and macrophage

The tumor-bearing mice of EL4-Ova were intratumorally injected with mVSVG-Exo (100 μg), Con-Exo (100 μg), wtVSVG-Exo (100 μg), or PBS on days 6 and 7 after tumor inoculation. On day 18, the extracted tumor tissues were enzymatically dissociated into single-cell suspensions with a tumor dissociation kit (Miltenyi Biotec). DCs or macrophages were magnetically enriched from single-cell suspensions using CD11c- or F4/80-specific magnetic beads (MACS isolation systems), respectively. DCs or macrophages were cocultured with OT-I cells isolated from C57BL/6-Tg(TcraTcrb)1100Mjb/J mice in a 1:5 ratio for 72 hours. The level of IFN-γ in cell supernatants was evaluated with the Mouse IFN-γ Quantikine ELISA Kit (R&D Systems).

IFN-γ production analysis

The tumor-bearing mice of EL4-Ova were intratumorally injected with mVSVG-Exo (100 μg), Con-Exo (100 μg), wtVSVG-Exo (100 μg), or PBS on days 6 and 7 after tumor inoculation. On day 10, 1×10^6 splenocytes isolated from each mouse were seeded to a 24-well dish and challenged with the Ova peptide (10 μg ml^{-1}) (SIINFEKL) at 37°C for 24 hours. The β-gal; TPHPARIGL and gp70; SPSYVYHQF peptides were used as negative peptides. To evaluate whether the formation of tumor-specific immunity is formed, the IFN-γ Quantikine ELISA Kit (R&D Systems) was used to measure the quantity of IFN-γ in the growth medium.

IFN-β production analysis

BMDCs (5×10^5) seeded in 96-well dishes were treated with mVSVG-Exo (50 μg ml^{-1}), Con-Exo (50 μg ml^{-1}), wtVSVG-Exo (50 μg ml^{-1}), or PBS for 24 hours at 37°C. To preblock the TLR4 receptor, BMDCs were pretreated with anti-TLR4 antibodies (clone MTS510, 16-9924-82, 10 μg ml^{-1}) for 1 hour before treatment of exosomes. To evaluate whether the type I IFN–related response was formed, a Quantikine ELISA for mouse IFN-β immunoassay (R&D Systems) was used to measure the quantity of IFN-β in the growth medium.

CD8 or PD-L1 immunofluorescence staining

Tumor tissues were obtained from the tumor-bearing mice of EL4-Ova on day 18 after the indicated treatment, embedded in OCT (Optimal Cutting Temperature) compound (Leica Biosystems) in a cryomold, and sectioned with a rotary microtome (at 10 μm). To remove nonspecific binding, sections were preblocked with PBS containing 3% BSA (Affymetrix) for 2 hours. The sections were then labeled at 4°C for overnight with CD8α (clone: 53-6.7) and PD-L1 (clone: 10F.9G2) antibodies. The next day, the sections washed with PBS and labeled with an Alexa Fluor 488–conjugated secondary antibody (Jackson ImmunoResearch). Purified rat IgG2a isotype control antibody (clone: R35-95) was used as a control. A fluorescence microscope (Nikon) was used to detect the CD8 or PD-L1 signals. The ImageJ program (National Institutes of Health) was used for quantifying the number of CD8$^+$ T cells per mm^2 (10 to 12 separate areas of three different tumors per group).

Measurement of intratumoral pH

BALB/c mice were implanted in the left flank with 1×10^6 CT26 cells. After the tumor reached an average size of 100 to 200 mm^3, pH 7.4 of PBS solution was administered via intratumoral injection. The intratumoral pH was measured with a pH meter (Thermo Fisher Scientific) with needles (Medical & Research Equipment Ltd., MI-407B) at the indicated times according to the manufacturer's instructions. Briefly, after calibrating the pH meter with a micro-electrode, a central hole was drilled into the tumor. Then, the reference electrode and pH measuring electrode were placed inside the tumor tissues and pH measurement was performed.

Cellular cytotoxicity analysis

To measure tumor cell toxicity, CCK-8 assay (Dojindo Laboratory) was performed. EL4-Ova or 4T1-Luc (5×10^3) fused with 50 μg of mVSVG-Exo was seeded at 96-well plates at 37°C for 24 hours. After 24 hours, 10 μl of CCK-8 solution was added to each well and then cell viability was evaluated with a microplate reader (SpectraMax 34, Molecular Devices).

Flow cytometry

Single-cell suspensions were preblocked with FcR antibody (clone: 2.4G2) and then labeled with fluorescence-conjugated antibodies according to the manufacturer's instructions. The data were analyzed using the FlowJo software (Tree Star). For intracellular cytokine staining of CD8$^+$ T cells, single cells of tumor tissues were resuspended in BD Cytofix/Cytoperm solution (BD Biosciences) for 30 min at 4°C and then labeled with the following fluorescence-conjugated antibodies: anti–IFN-γ (clone: XMG1.2, 505807), anti–TNF-α (clone: MP6-XT22, 506305), and anti–IL-2 (clone: JES6-5H4, 503807) in 1× Perm/Wash buffer (BD Biosciences). For calculating the relative MFI, the MFI for each sample was divided by the MFI of the control sample. The relative MFI in Fig. 1C and figs. S1 (D and F), S2, and S3A was calculated by dividing the MFI for each sample by the average MFI of pH 7.4 samples. The relative MFI in Fig. 2E was calculated by dividing the MFI for each sample (mCh$^+$, CD45$^+$, CD31$^+$, or CD90.2$^+$) by the average MFI of matched control samples (mCh$^+$,

$CD45^+$, $CD31^+$, or $CD90.2^+$). The relative MFI in Figs. 3B and 4F and fig. S7B was calculated by dividing the MFI for each sample by the average MFI of control samples.

Statistical analysis

The size of the sample was selected based on the relevant literature. Student's *t* test using the SigmaPlot 10.0 software was used for comparing between two groups. The significance of differences among more than two groups was decided by one-way analysis of variance (ANOVA) followed by Tukey's post hoc test with Prism 5.0 (GraphPad). The statistical comparison of survival data estimated by Kaplan-Meier analysis was evaluated using the log-rank test with Prism 5.0 (GraphPad). All error bars are presented by SD. P values < 0.05 were determined to be statistically significant, and P values are further specified in the figure legends.

SUPPLEMENTARY MATERIALS

Supplementary material for this article is available at http://advances.sciencemag.org/cgi/content/full/6/27/eaaz2083/DC1

View/request a protocol for this paper from *Bio-protocol*.

REFERENCES AND NOTES

1. R. W. Jenkins, D. A. Barbie, K. T. Flaherty, Mechanisms of resistance to immune checkpoint inhibitors. *Br. J. Cancer* **118**, 9–16 (2018).
2. M. Yarchoan, A. Hopkins, E. M. Jaffee, Tumor mutational burden and response rate to PD-1 inhibition. *N. Engl. J. Med.* **377**, 2500–2501 (2017).
3. O. V. Matveeva, Z. S. Guo, S. A. Shabalina, P. M. Chumakov, Oncolysis by paramyxoviruses: Multiple mechanisms contribute to therapeutic efficiency. *Mol. Ther. Oncolytics* **2**, 15011 (2015).
4. M. Kobayashi, Viral xenogenization of intact tumor cells. *Adv. Cancer Res.* **30**, 279–299 (1979).
5. O. Franzese, F. Torino, M. P. Fuggetta, A. Aquino, M. Roselli, E. Bonmassar, A. Giuliani, S. D'Atri, Tumor immunotherapy: Drug-induced neoantigens (xenogenization) and immune checkpoint inhibitors. *Oncotarget* **8**, 41641–41669 (2017).
6. H. Valadi, K. Ekström, A. Bossios, M. Sjöstrand, J. J. Lee, J. O. Lötvall, Exosome-mediated transfer of mRNAs and microRNAs is a novel mechanism of genetic exchange between cells. *Nat. Cell Biol.* **9**, 654–659 (2007).
7. E. Cho, G.-H. Nam, Y. Hong, Y. K. Kim, D.-H. Kim, Y. Yang, I.-S. Kim, Comparison of exosomes and ferritin protein nanocages for the delivery of membrane protein therapeutics. *J. Control. Release* **279**, 326–335 (2018).
8. E. Koh, E. J. Lee, G.-H. Nam, Y. Hong, E. Cho, Y. Yang, I.-S. Kim, Exosome-SIRPα, a CD47 blockade increases cancer cell phagocytosis. *Biomaterials* **121**, 121–129 (2017).
9. D. K. Miller, J. W. Gillard, P. J. Vickers, S. Sadowski, C. Léveillé, J. A. Mancini, P. Charleson, R. A. F. Dixon, A. W. Ford-Hutchinson, R. Fortin, J. Y. Gauthier, J. Rodkey, R. Rosen, C. Rouzer, I. S. Sigal, C. D. Strader, J. F. Evans, Identification and isolation of a membrane protein necessary for leukotriene production. *Nature* **343**, 278–281 (1990).
10. C. M. Niemeyer, Nanoparticles, proteins, and nucleic acids: Biotechnology meets materials science. *Angew. Chem. Int. Ed.* **40**, 4128–4158 (2001).
11. Y. Yang, Y. Hong, E. Cho, G. B. Kim, I.-S. Kim, Extracellular vesicles as a platform for membrane-associated therapeutic protein delivery. *J. Extracell. Vesicles* **7**, 1440131 (2018).
12. Y. Yang, Y. Hong, G.-H. Nam, J. H. Chung, E. Koh, I.-S. Kim, Virus-mimetic fusogenic exosomes for direct delivery of integral membrane proteins to target cell membranes. *Adv. Mater.* **29**, 1605604 (2017).
13. P. Oyston, K. Robinson, The current challenges for vaccine development. *J. Med. Microbiol.* **61**, 889–894 (2012).
14. A. L. Cunningham, N. Garçon, O. Leo, L. R. Friedland, R. Strugnell, B. Laupèze, M. Doherty, P. Stern, Vaccine development: From concept to early clinical testing. *Vaccine* **34**, 6655–6664 (2016).
15. G. Redelman-Sidi, M. S. Glickman, B. H. Bochner, The mechanism of action of BCG therapy for bladder cancer—A current perspective. *Nat. Rev. Urol.* **11**, 153–162 (2014).
16. A. Monie, C.-F. Hung, R. Roden, T.-C. Wu, Cervarix: A vaccine for the prevention of HPV 16, 18-associated cervical cancer. *Biol. Theory* **2**, 97–105 (2008).
17. M. H. Moehler, M. Zeidler, V. Wilsberg, J. J. Cornelis, T. Woelfel, J. Rommelaere, P. R. Galle, M. Heike, Parvovirus H-1-induced tumor cell death enhances human immune response in vitro via increased phagocytosis, maturation, and cross-presentation by dendritic cells. *Hum. Gene Ther.* **16**, 996–1005 (2005).
18. B. Sangiuliano, N. M. Pérez, D. F. Moreira, J. E. Belizário, Cell death-associated molecular-pattern molecules: Inflammatory signaling and control. *Mediators Inflamm.* **2014**, 821043 (2014).
19. D. Zhu, D. H. Lam, Y. I. Purwanti, S. L. Goh, C. Wu, J. Zeng, W. Fan, S. Wang, Systemic delivery of fusogenic membrane glycoprotein-expressing neural stem cells to selectively kill tumor cells. *Mol. Ther.* **21**, 1621–1630 (2013).
20. L. Feng, Z. Dong, D. Tao, Y. Zhang, Z. Liu, The acidic tumor microenvironment: A target for smart cancer nano-theranostics. *Natl. Sci. Rev.* **5**, 269–286 (2018).
21. D. Finkelshtein, A. Werman, D. Novick, S. Barak, M. Rubinstein, LDL receptor and its family members serve as the cellular receptors for vesicular stomatitis virus. *Proc. Natl. Acad. Sci. U.S.A.* **110**, 7306–7311 (2013).
22. S. Shelly, N. Lukinova, S. Bambina, A. Berman, S. Cherry, Autophagy is an essential component of Drosophila immunity against vesicular stomatitis virus. *Immunity* **30**, 588–598 (2009).
23. G.-H. Nam, E. J. Lee, Y. K. Kim, Y. Hong, Y. Choi, M.-J. Ryu, J. Woo, Y. Cho, D. J. Ahn, Y. Yang, I.-C. Kwon, S.-Y. Park, I.-S. Kim, Combined Rho-kinase inhibition and immunogenic cell death triggers and propagates immunity against cancer. *Nat. Commun.* **9**, 2165 (2018).
24. N. Wathelet, M. Moser, Role of dendritic cells in the regulation of antitumor immunity. *Oncoimmunology* **2**, e23973 (2013).
25. B. Sauter, M. L. Albert, L. Francisco, M. Larsson, S. Somersan, N. Bhardwaj, Consequences of cell death: Exposure to necrotic tumor cells, but not primary tissue cells or apoptotic cells, induces the maturation of immunostimulatory dendritic cells. *J. Exp. Med.* **191**, 423–434 (2000).
26. H. Shen, B. M. Tesar, W. E. Walker, D. R. Goldstein, Dual signaling of MyD88 and TRIF is critical for maximal TLR4-induced dendritic cell maturation. *J. Immunol.* **181**, 1849–1858 (2008).
27. S. N. Lester, K. Li, Toll-like receptors in antiviral innate immunity. *J. Mol. Biol.* **426**, 1246–1264 (2014).
28. P. Georgel, Z. Jiang, S. Kunz, E. Janssen, J. Mols, K. Hoebe, S. Bahram, M. B. A. Oldstone, B. Beutler, Vesicular stomatitis virus glycoprotein G activates a specific antiviral Toll-like receptor 4-dependent pathway. *Virology* **362**, 304–313 (2007).
29. K. Abiko, N. Matsumura, J. Hamanishi, N. Horikawa, R. Murakami, K. Yamaguchi, Y. Yoshioka, T. Baba, I. Konishi, M. Mandai, IFN-γ from lymphocytes induces PD-L1 expression and promotes progression of ovarian cancer. *Br. J. Cancer* **112**, 1501–1509 (2015).
30. K. Mimura, J. L. Teh, H. Okayama, K. Shiraishi, L.-F. Kua, V. Koh, D. T. Smoot, H. Ashktorab, T. Oike, Y. Suzuki, Z. Fazreen, B. R. Asuncion, A. Shabbir, W.-P. Yong, J. So, R. Soong, K. Kono, PD-L1 expression is mainly regulated by interferon gamma associated with JAK-STAT pathway in gastric cancer. *Cancer Sci.* **109**, 43–53 (2018).
31. D. Farquhar, J. Benvenuto, 1-Aryl-3,3-dimethyltriazenes: Potential central nervous system active analogues of 5-(3,3-dimethyl-1-triazeno)imidazole-4-carboxamide (DTIC). *J. Med. Chem.* **27**, 1723–1727 (1984).

Acknowledgments

Funding: This work was supported by a National Research Foundation of Korea (NRF) grant funded by the Korean government (MSIT) (2019R1A2B5B03004360 and 2017R1A3B1023418), by the KU-KIST School Project, and by the KIST Institutional Program. **Author contributions:** All authors have given approval to the final version of the manuscript. Y.Y., I.C.K., and I.-S.K. designed experiments. G.B.K., G.-H.N., Y.H., and Y.C. performed experiments. G.B.K., G.-H.N., Y.H., J.W., and Y.Y. analyzed the data. G.B.K., G.-H.N., Y.Y., and I.-S.K. wrote the manuscript. **Competing interests:** The authors declare that they have no competing interests. **Data and materials availability:** All data needed to evaluate the conclusions in the paper are present in the paper and/or the Supplementary Materials. Additional data related to this paper may be requested from the authors.

Submitted 22 August 2019
Accepted 15 May 2020
Published 1 July 2020
10.1126/sciadv.aaz2083

Citation: G. B. Kim, G.-H. Nam, Y. Hong, J. Woo, Y. Cho, I. C. Kwon, Y. Yang, I.-S. Kim, Xenogenization of tumor cells by fusogenic exosomes in tumor microenvironment ignites and propagates antitumor immunity. *Sci. Adv.* **6**, eaaz2083 (2020).